

The Effect of Molding Pressure on Electrochemical Properties of the La-Mg-Ni-Based Composite Hydrogen Storage Alloy Electrodes

Liqiang Ji^{1,*}, Yonggang Yang¹, Xilin Zhu¹, Lili Liu³, Baozhong Liu^{1,2,*}

¹ Inner Mongolia Rare Earth Ovonic Hydrogen Storage Alloy Corporation Limited, Baotou 014030, China

² School of Material Science and Engineering, Henan Polytechnic University, Jiaozuo 454000, China

³ College of Material and Metallurgy, Inner Mongolia University of Science and Technology, Baotou 014030, China

*E-mail: jlq1231@126.com; b_z_liu@163.com

Received: 1 November 2012 / Accepted: 30 November 2012 / Published: 1 January 2013

The microstructures and electrochemical properties of the La-Mg-Ni-based hydrogen storage alloy electrodes prepared under different molding pressure (P) have been studied systematically by Physical Property Measurement System (PPMS), Metallurgical Microscope and electrochemical measurements. Specific resistance of the composite alloy electrodes monotonously decreases from $2.06 \times 10^{-6} \Omega \cdot \text{m}$ ($P = 200$ MPa) to $0.40 \times 10^{-6} \Omega \cdot \text{m}$ ($P = 1000$ MPa). Maximum discharge capacity of alloy electrode first increases from 371 mAh/g ($P = 200$ MPa) to 398 mAh/g ($P = 300$ MPa), and then decrease to 384 mAh/g ($P = 1000$ MPa). The HRD of the alloy electrodes first increases and then decreases with increasing molding pressure, and the best high-rate dischargeability can be obtained when P is 400 MPa. The I_0 value decreases from 524.00 mA/g ($P = 300$ MPa) to 356.85 mA/g ($P = 1000$ MPa). The I_L values first increase from 1124 mA/g ($P = 300$ MPa) to 1192 mA/g ($P = 400$ MPa) and then decrease to 777 mA/g ($P = 1000$ MPa). The optimum P value in our experiment is 400 MPa.

Keywords: Hydrogen storage alloy; High pressure; Electrochemical properties; Kinetics

1. INTRODUCTION

Nickel/metal-hydride (Ni/MH) secondary batteries have been widely by virtue of several of their advantages, such as high energy density, high rate capacity, good overdischarge capability, containing no poisonous heavy metal and no electrolyte consumption during charge/discharge cycling[1-4]. Many attempts have been made to improve the overall properties of hydrogen storage alloys as negative electrode materials in Ni/MH batteries, and a series of new type hydrogen storage

alloys have been discovered [5-8]. In recent years the investigations of hydrogen storage alloy mainly focus on optimizing the alloy component, surface modification and annealing treatment. Seo et al.[9] reported that the discharge capacity and activation of hydrogen storage capacity of $\text{LaNi}_{3.6}\text{Al}_{0.4}\text{Co}_{0.7}\text{Mn}_{0.3}\text{V}_y$ can be improved by adding V in the range 0.02-0.1, and high-rate dischargeability was also enhanced due to the improvement in kinetic performance. Chen [10] studied the effect of surface modification on electrochemical properties of the $\text{MnNi}_{4.0}\text{Co}_{0.6}\text{Al}_{0.3}$ alloy and found that the discharge capacity and HRD property was improved obviously. Pan[11] studied the structural and electrochemical properties of $\text{La}_{0.7}\text{Mg}_{0.3}(\text{Ni}_{0.85}\text{Co}_{0.15})_x$ ($x=3.0-5.0$) hydrogen storage alloys, and the results showed that the structures of the alloys changed obviously with increasing x value. Jin [12] studied annealing treatment can make the $\text{ML}_{1-x}\text{Mm}_x(\text{NiCoMnAl})_5$ alloy more homogeneous, and can effectively decrease lattice defect and stress inside the alloy particles. On the other hand, the electrochemical properties of the hydrogen storage alloy electrodes also depend on some factors in the electrode preparation[13-15]. Among those factors, the molding pressure is a very important. Up to date, few investigations on the relationship between electrochemical properties of alloy electrode and molding pressure has been reported.

In this work, the specific resistance, microstructure, charge/discharge characteristics and electrochemical kinetics of $\text{La}_{0.88}\text{Mg}_{0.12}\text{Ni}_{2.94}\text{Mn}_{0.12}\text{Co}_{0.56}\text{Al}_{0.2} + 10 \text{ wt.}\% \text{ Co}$ composite alloy electrodes with additive were investigated systematically.

2. EXPERIMENTAL PROCEDURES

The $\text{La}_{0.88}\text{Mg}_{0.12}\text{Ni}_{2.94}\text{Mn}_{0.12}\text{Co}_{0.56}\text{Al}_{0.2}$ alloys were prepared by induction melting under argon atmosphere (purity of La, Mg Ni, Co, Mn and Al are more than 99.9%). The prepared ingots were annealed at 1173 K for 8 h. Then they were mechanically crushed and ground into fine powders which were used for electrochemical test. 10 wt.% Co was added into the $\text{La}_{0.88}\text{Mg}_{0.12}\text{Ni}_{2.94}\text{Mn}_{0.12}\text{Co}_{0.56}\text{Al}_{0.2}$ alloys. After mixing the two kinds of alloy powders homogeneously, we can obtain the $\text{La}_{0.88}\text{Mg}_{0.12}\text{Ni}_{2.94}\text{Mn}_{0.12}\text{Co}_{0.56}\text{Al}_{0.2} + 10 \text{ wt.}\% \text{ Co}$ composite powders. The well-mixed composite alloy powders and carbonyl nickel powder in weight ratio of 1:5 were pressed into pellets which had the diameter of 25 mm and thickness of 1.5 mm under different pressure (200 MPa, 300 MPa, 400 MPa, 800 MPa and 1000 MPa respectively) in the hydraulic press extruder. Finally, the $\text{La}_{0.88}\text{Mg}_{0.12}\text{Ni}_{2.94}\text{Mn}_{0.12}\text{Co}_{0.56}\text{Al}_{0.2} + 10 \text{ wt.}\% \text{ Co}$ composite alloy electrodes were obtained for testing.

The specific resistance of composite alloy electrodes prepared under different molding pressure was carried out by Physical Property Measurement System (PPMS) at normal temperature and the micro-structure of the composite alloy electrodes was observed by AXIOVERT200MAT Metallurgical Microscope. The electrochemical studies were carried out in half-cell consisting of MH electrode, $\text{Ni}(\text{OH})_2/\text{NiOOH}$ electrode and Hg/HgO electrode.

The charge/discharge characteristics at different current of the alloy electrodes were tested by the DC-5 battery testing instrument. Each electrode was charged at 146 mA/g for 4.5h followed by a 10min rest and then discharged at 73 mA/g to the cut-off potential of -0.6V versus the Hg/HgO

reference electrode. The linear polarization curves and the anodic polarization curves of the electrodes were measured on the ZF-9 potentiostat at 50% depth of discharge (DOD) respectively at 298K.

3. RESULTS AND DISCUSSION

3.1 Metallographic structure

Fig. 1 shows the metallograph of the $\text{La}_{0.88}\text{Mg}_{0.12}\text{Ni}_{2.94}\text{Mn}_{0.12}\text{Co}_{0.56}\text{Al}_{0.2} + 10\text{wt.}\% \text{Co}$ composite alloys under 300 MPa and 800 MPa molding pressure. It can be seen that the particles inside the composite alloys distribute in an incompact arrangement and most particles are disjunct when the molding pressure is 300 MPa. When the molding pressure increases to 800 MPa, the particles inside the composite alloy electrodes distribute more compactly and begin to deform and conglutinate, which result in the increase of the contact area among the particles and reducing the specific resistance, however, the interspaces among the particles decreases, so it may be difficult for the electrolyte to saturate into or out of the alloy electrodes.

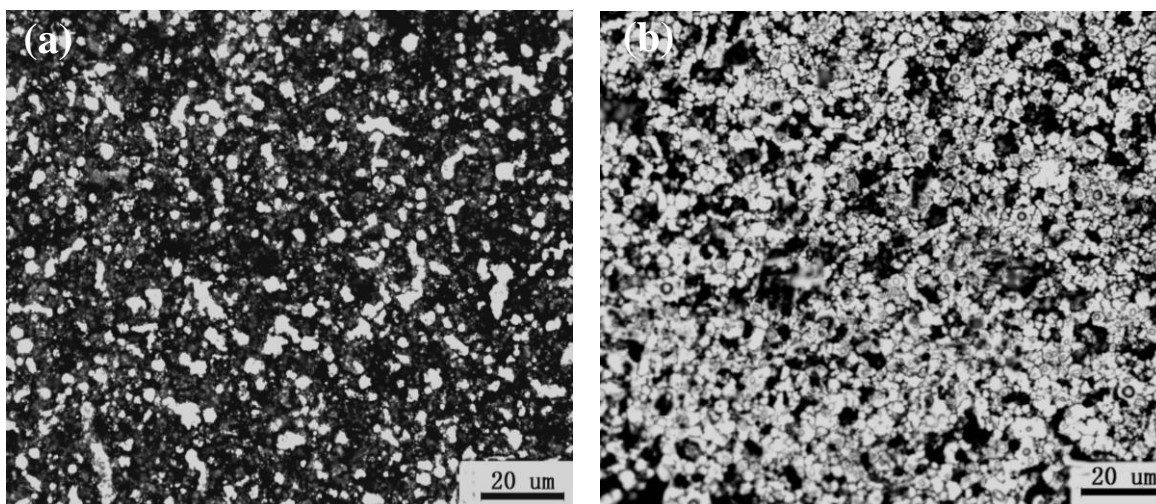


Figure 1. Metallograph of $\text{La}_{0.88}\text{Mg}_{0.12}\text{Ni}_{2.94}\text{Mn}_{0.12}\text{Co}_{0.56}\text{Al}_{0.2} + 10 \text{ wt.}\% \text{Co}$ composite electrodes under different molding pressure (a) 300 MPa; (b) 800 MPa

3.2 Specific resistance

Fig. 2 shows the specific resistance of the $\text{La}_{0.88}\text{Mg}_{0.12}\text{Ni}_{2.94}\text{Mn}_{0.12}\text{Co}_{0.56}\text{Al}_{0.2} + 10 \text{ wt.}\% \text{Co}$ composite alloy at different pressure. It can be seen that the specific resistance of the composite alloy decreases from $2.06 \times 10^{-6} \Omega \cdot \text{m}$ ($P = 200 \text{ MPa}$) to $0.40 \times 10^{-6} \Omega \cdot \text{m}$ ($P = 1000 \text{ MPa}$) monotonically with increasing molding pressure, which may be ascribed to following factors. Firstly, the alloy becomes more compact and the pore size inside the alloy becomes fewer, which lead to the increase of the

interface area among the particles inside the composite alloys. Secondly, high pressure may cause the broken oxide film on the surface, which is beneficial to the conductivity.

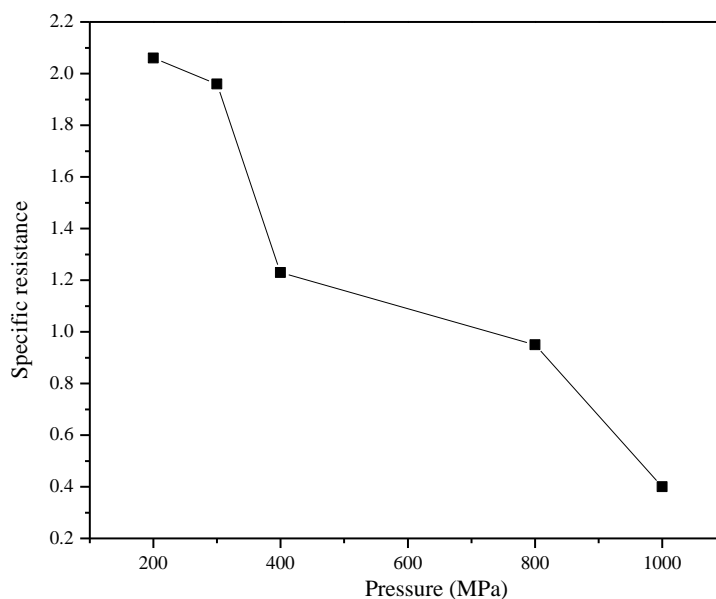


Figure 2. Specific resistance of $\text{La}_{0.88}\text{Mg}_{0.12}\text{Ni}_{2.94}\text{Mn}_{0.12}\text{Co}_{0.56}\text{Al}_{0.2} + 10 \text{ wt.}\% \text{ Co}$ composite electrodes

3.3 Activation and discharge capacity

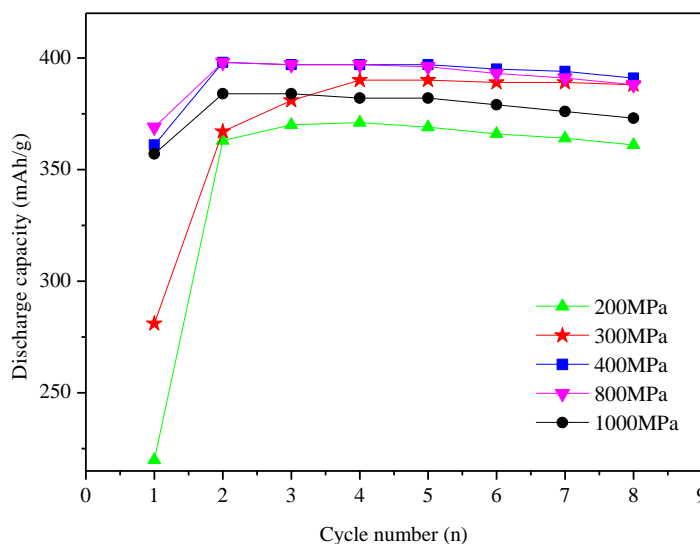


Figure 3. Activation and discharge capacity curve of $\text{La}_{0.88}\text{Mg}_{0.12}\text{Ni}_{2.94}\text{Mn}_{0.12}\text{Co}_{0.56}\text{Al}_{0.2} + 10 \text{ wt.}\% \text{ Co}$ composite electrodes under different pressure

Fig. 3 shows the activation and discharge capacity curves of the $\text{La}_{0.88}\text{Mg}_{0.12}\text{Ni}_{2.94}\text{Mn}_{0.12}\text{Co}_{0.56}\text{Al}_{0.2} + 10 \text{ wt.}\% \text{ Co}$ composite alloy electrodes at different molding pressure. It can be seen that the activation property of the composite alloy electrodes is improved with

the increase of the molding pressure. When P is 200 MPa or 300 MPa, the composite electrodes can be activated after 3 cycles. When molding pressure is more than 400 MPa, the 2 cycles are need to active the alloy electrode. In general, the activity property of alloy electrode is related the oxide film of alloy particles. The improvement of activity property should be ascribed to the broken oxide film under higher molding pressure.

Table 1. Electrochemical properties of $\text{La}_{0.88}\text{Mg}_{0.12}(\text{Ni}_{2.94}\text{Mn}_{0.12}\text{Co}_{0.56}\text{Al}_{0.2}) + 10 \text{ wt.}\% \text{ Co}$ composite electrodes under different molding pressure

P (MPa)	N_a (n)	C_{\max} (mAh/g)	HRD ₁₅₀₀ ^a (%)
200	4	371	18.86
300	4	390	21.28
400	2	398	39.14
500	2	395	32.11
600	2	384	26.08

^a The high-rate dischargeability at the discharge current density of 1500 mA/g.

Table 1 gives the maximum discharge capacity (C_{\max}) of the $\text{La}_{0.88}\text{Mg}_{0.12}\text{Ni}_{2.94}\text{Mn}_{0.12}\text{Co}_{0.56}\text{Al}_{0.2} + 10 \text{ wt.}\% \text{ Co}$ composite alloy electrodes at different molding pressure. Clearly the C_{\max} of alloy electrode first increases from 371 mAh/g ($P = 200$ MPa) to 398 mAh/g ($P = 300$ MPa), and then decrease to 384 mAh/g ($P = 1000$ MPa). As above-mentioned, the specific resistance decreases with the increase of the molding pressure. The decrease of specific resistance will lead the increase the electronic conductivity, which will enhance the discharge property and increase the discharge capacity. Unfortunately, Meng et al.[16] reported that higher molding pressure caused the capillary of the alloy electrodes to become extremely fine, it is difficult for the electrolyte to saturate into or out of the alloy electrodes, and the active element inside the cathode can not be used effectively, which degrades the discharge capacity. Obviously, the increase of electronic conductivity resulted from the increase of molding pressure are favorable for the maximum discharge capacity, but the decrease of active element is unfavorable. Therefore, it is reasonable to assume that, with molding pressure of lower than a certain amount, the favorable effect is dominant and will cause an increase of the maximum discharge capacity. However, when molding pressure exceeds the critical content, the unfavorable effect will become dominant and will give rise to the decrease of the maximum discharge capacity. The critical molding pressure is 400 MPa for $\text{La}_{0.88}\text{Mg}_{0.12}\text{Ni}_{2.94}\text{Mn}_{0.12}\text{Co}_{0.56}\text{Al}_{0.2} + 10 \text{ wt.}\% \text{ Co}$ composite alloy electrodes.

3.4 High-rate dischargeability (HRD) and electrochemical kinetics

Fig. 4 shows the HRD curves of $\text{La}_{0.88}\text{Mg}_{0.12}\text{Ni}_{2.94}\text{Mn}_{0.12}\text{Co}_{0.56}\text{Al}_{0.2} + 10 \text{ wt.}\% \text{ Co}$ composite electrodes under different molding pressure. It can be seen that the HRD of the alloy electrodes first increased and then decreased with increasing molding pressure. The alloy electrode ($P = 400$ MPa) exhibits the best high-rate dischargeability. Table 2 also lists the HRD values (HRD₁₅₀₀) of the alloy

electrodes when the discharge current is 1500 mA/g. with increasing molding pressure, the HRD₁₅₀₀ value first increased from 18.86% ($P = 200$ MPa) to 39.14% ($P = 400$ MPa) and then decreased to 15.03% ($P = 1000$ MPa).

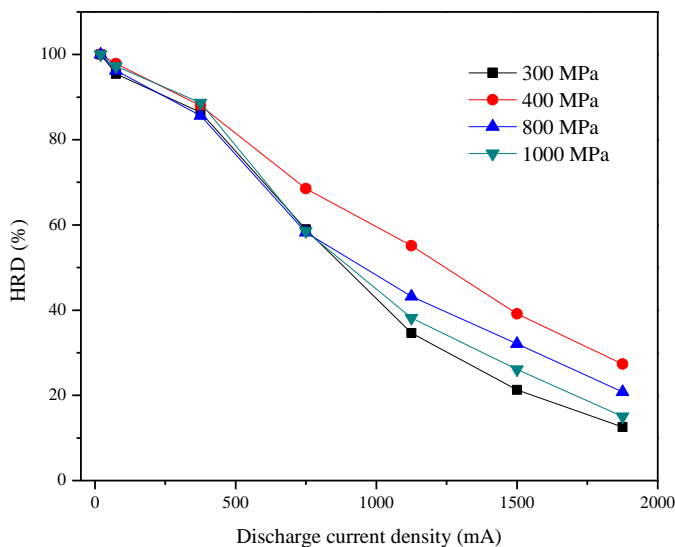


Figure 4. HRD of $\text{La}_{0.88}\text{Mg}_{0.12}\text{Ni}_{2.94}\text{Mn}_{0.12}\text{Co}_{0.56}\text{Al}_{0.2} + 10$ wt.% Co composite electrodes under different pressure

It is well known that the HRD of the metal hydride electrodes are influenced mainly by the charge-transfer kinetics at the electrode/electrolyte interface and hydrogen diffusion rate in the bulk of alloy[17]. The exchange current density I_0 of alloy electrode is commonly used to characterize the catalytic activity for charge-transfer reaction at the electrode/electrolyte interface, and limited current density (I_L) is used to characterize hydrogen diffusion rate in the bulk of alloy. In order to obtain I_0 and I_L , linear polarization and potential-step experiment are performed on these alloy electrodes.

Fig. 5 shows the linear polarization curves of $\text{La}_{0.88}\text{Mg}_{0.12}\text{Ni}_{2.94}\text{Mn}_{0.12}\text{Co}_{0.56}\text{Al}_{0.2} + 10$ wt.% Co composite electrodes under different pressure at 50% DOD and 298K. The polarization resistance (R_p) is calculated through estimating the slopes of linear polarization curves and listed in Table 2. R_p value increases from 49.2 mΩ g ($P = 300$ MPa) to 72.4 mΩ g ($P = 1000$ MPa). Furthermore, the exchange current density I_0 of alloy electrode is calculated from the slopes of polarization curves by the following equation [18] and listed in Table 2.

$$I_0 = \frac{RT}{FR_p} \tag{1}$$

Where R is the gas constant, T is the absolute temperature, F is the Faraday constant, R_p is the polarization resistance. Clearly the I_0 value decreases from 524.00 mA/g ($P = 300$ MPa) to 356.85 mA/g ($P = 1000$ MPa). It is well known that the I_0 is related to the surface activity of alloy electrode[18]. Increasing pressure will cause the deformation and conglutination of alloy particle and

additive[12], which is detrimental to the electrocatalytic activity of alloy surface, and then give rise to the increase of R_p and the decrease of I_0 . Thus, the I_0 value decreases with increasing molding pressure in our experiments.

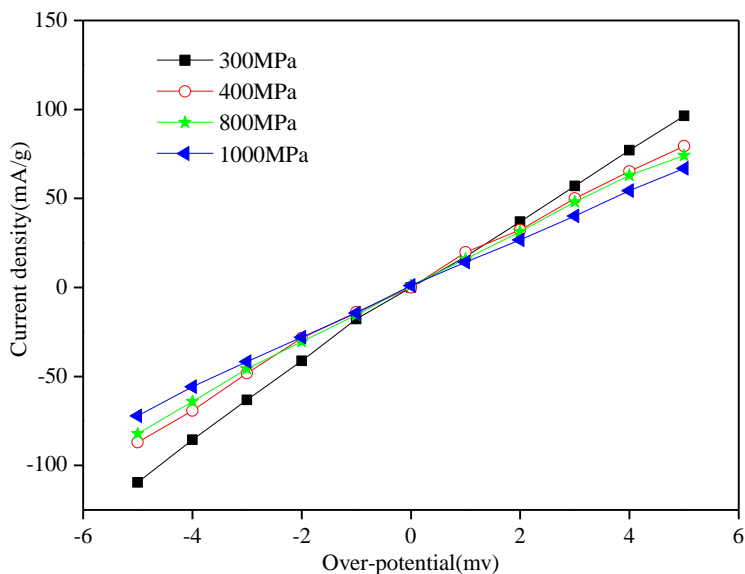


Figure 5. Exchange current density curve of $\text{La}_{0.88}\text{Mg}_{0.12}\text{Ni}_{2.94}\text{Mn}_{0.12}\text{Co}_{0.56}\text{Al}_{0.2} + 10 \text{ wt.}\% \text{ Co}$ composite electrodes under different pressure

Table 2. Electrochemical kinetics of $\text{La}_{0.88}\text{Mg}_{0.12}\text{Ni}_{2.94}\text{Mn}_{0.12}\text{Co}_{0.56}\text{Al}_{0.2} + 10 \text{ wt.}\% \text{ Co}$ composite electrodes

P (MPa)	R_p ($\text{m}\Omega \text{ g}$)	I_0 (mA/g)	I_L (mA/g)
300	49.2	524.0	1124
400	63.6	427.4	1192
800	60.3	405.7	784
1000	72.4	356.9	777

Fig. 6 shows the anodic polarization of the $\text{La}_{0.88}\text{Mg}_{0.12}\text{Ni}_{2.94}\text{Mn}_{0.12}\text{Co}_{0.56}\text{Al}_{0.2} + 10 \text{ wt.}\% \text{ Co}$ composite alloy electrodes under different molding pressure at 50 % DOD and 298 K. It can be seen that the anodic current density increases with increasing overpotential and finally reaches a limiting value defined as the limiting current density I_L [19]. In general, the limiting current density I_L represents the hydrogen diffusivity in the bulk of the alloys, that is, the larger the I_L value, the faster is the diffusion of the hydrogen atoms in the alloys [20]. The I_L values are also summarized in Table 2. With increasing molding pressure, the I_L value first increases from 1124 mA/g ($P = 300 \text{ MPa}$) to 1192 mA/g ($P = 400 \text{ MPa}$) and then decreases to 777 mA/g ($P = 1000 \text{ MPa}$), which indicates that the hydrogen diffusivity rate in the composite alloy electrodes first increases and then decreases. With increasing molding pressure, the surface oxide film is easily broken [12] and the metallic Ni and Co on

the alloy surface increase, which makes hydrogen diffuse from the bulk to the surface more easily. This is beneficial to the hydrogen diffusion coefficient. Unfortunately, the additive enwraps the alloy particle compactly, which decrease the hydrogen diffusion channel and give rise to the decrease of hydrogen diffusion coefficient. The highest hydrogen diffusion rate is obtained when molding pressure is 400 MPa, which is ascribed to the combined effect of beneficial and unbeneficial factors.

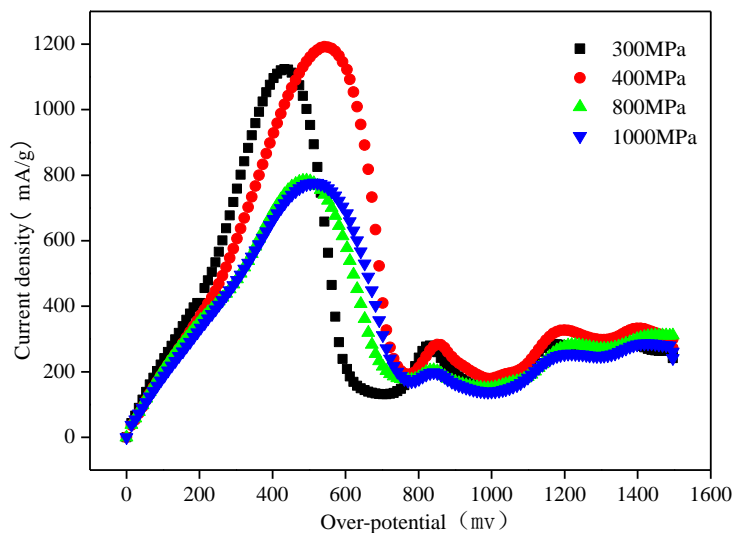


Figure 6. Anodic polarization curve of $\text{La}_{0.88}\text{Mg}_{0.12}\text{Ni}_{2.94}\text{Mn}_{0.12}\text{Co}_{0.56}\text{Al}_{0.2} + 10 \text{ wt.}\% \text{Co}$ composite electrodes under different pressure

4. CONCLUSIONS

The $\text{La}_{0.88}\text{Mg}_{0.12}\text{Ni}_{2.94}\text{Mn}_{0.12}\text{Co}_{0.56}\text{Al}_{0.2} + 10 \text{ wt.}\% \text{Co}$ composite alloy electrodes under different molding pressure were prepared. Specific resistance of the composite alloy electrodes reduced from $2.06 \times 10^{-6} \Omega \cdot \text{m}$ ($P = 200 \text{ MPa}$) to $0.40 \times 10^{-6} \Omega \cdot \text{m}$ ($P = 1000 \text{ MPa}$) monotonously. The C_{max} of alloy electrode first increases from 371 mAh/g ($P = 200 \text{ MPa}$) to 398 mAh/g ($P = 300 \text{ MPa}$), and then decrease to 384 mAh/g ($P = 1000 \text{ MPa}$). the HRD of the alloy electrodes first increased and then decreased with increasing molding pressure. The alloy electrode ($P = 400 \text{ MPa}$) exhibits the best high-rate dischargeability. The I_0 value decreases from 524.00 mA/g ($P = 300 \text{ MPa}$) to 356.85 mA/g ($P = 1000 \text{ MPa}$). The I_L values first increase from 1124 mA/g ($P = 300 \text{ MPa}$) to 1192 mA/g ($P = 400 \text{ MPa}$) and then decrease to 777 mA/g ($P = 1000 \text{ MPa}$).

References

1. B. Liao, Y.Q. Lei, L.X. Chen, G.L. Lu, H.G. Pan and Q.D. Wang, *J. Alloys Compd.*, 376 (2004) 186
2. S. Bliznakov, E. Lefterova, N. Dimitrov, K. Petrov and A. Popov, *J. Power Sources*, 176 (2008) 381

3. S.R. Ovshinsky, M.A. Fetcenko and J. Ross, *Science*, 260 (1993) 176
4. X.B. Zhang, D.Z. Sun, W.Y. Yin, Y.J. Chai and M.S. Zhao, *Chem Phys Chem*, 6 (2005) 520
5. M. Latroche, Y. Chabre, A. Percheron-Guegan, O. Isnard and B. Knop, *J. Alloys Comp.*, 330-332 (2002) 787
6. B. Liu, M. Hu, Y. Fan, L. Ji, X. Zhu and A. Li, *Electrochim. Acta*, 69 (2012) 384
7. S. Bliznakov, E. Lefterova, N. Dimitrov, K. Petrov and A. Popov, *J. Power Sources*, 176 (2008) 381
8. X. Tian, X.D. Liu, J. Xu, H.W. Feng, B. Chi, L.H. Huang and S.F. Yan, *Int. J. Hydrogen Energy*, 34 (2009) 2295
9. C. Y. Seo, S. J. Choi, J. Choi, C. N. Park and J. Y. Lee, *Int. J. Hydrogen Energy*, 28 (2003) 967
10. W. X. Chen, J. Q. Qi, Y. Chen, C. P. Chen, Q. D. Wang and J. M. Zhou, *J. Alloys Comp.*, 293-295 (1999) 728
11. H. G. Pan, Y. F. Liu, M. X. Gao, Y. F. Zhu and Y. Q. Lei, *Int. J. Hydrogen Energy*, 28 (2003) 1219
12. H. M. Jin, G. X. Li, R. K. Wang, C. Q. Wang, Z. L. Zhang and L. H. Sun, *Chin. J. Power Sources*, 21 (1997) 14
13. Z. H. Ma, J. F. Qiu, L. X. Chen and Y. Q. Lei, *J. Power Sources*, 125 (2004) 267
14. P. Li, Y. H. Zhang, X. L. Wang, Y. F. Lin and Qu X.H., *J. Power Sources*, 124 (2003) 285
15. T. Ise, T. Hamamatsu, T. Imoto, M. Nogami and S. Nakahori, *J. Power Sources*, 92 (2001) 81
16. M. W. Meng, C. M. Liu and X. M. Deng, *Chin. J. Power Sources*, 22 (1998) 155
17. B. Liu, G. Fan, Y. Wang, G. Mi, Y. Wu and L. Wang, *Int. J. Hydrogen Energy*, 33 (2008) 5801
18. P. Notten and P. Hokkeling, *J. Electrochem. Soc.*, 138 (1991) 1877
19. Y.F. Liu, H.G. Pan, M. X. Gao, R. Li, X. Z. Sun, Y. Q. Lei, *J. Alloys Compd.*, 388 (2005) 109
20. B.V. Ratnakumar, C. Witham, R.C. Bowman Jr., A. Hightower, B. Fultz, *J. Electrochem. Soc.*, 143 (1996) 2578